Pair density wave in the doped three-band Hubbard model on two-leg square cylinders

Hong-Chen Jiang

Pair density wave in doped three-band Hubbard model on two-leg square cylinders

Hong-Chen Jiang[*]

Stanford Institute for Materials and Energy Sciences,
SLAC National Accelerator Laboratory and Stanford University, Menlo Park, California 94025, USA

(Dated: May 23, 2023)

A pair density wave (PDW) is a superconducting (SC) state with spatially modulated order parameter. Although much is known about the properties of the PDW state, its realization in microscopic models with divergent susceptibility has been challenging. Here we report a density-matrix renormalization group study of a three-band Hubbard model (also known as the Emery model) for cuprates on long two-leg square cylinders. Upon light doping, we find that the ground state of the system is consistent with that of a PDW state with mutually commensurate and power-law SC, charge (CDW) and spin (SDW) density wave correlations. The SC correlations are dominant between neighboring Cu sites with d-wave pairing symmetry. Interestingly, we find that the near-neighbor interactions, especially the near-neighbor attractive V_{pd} interaction between neighboring Cu and oxygen sites, can notably enhance the SC correlations while simultaneously suppressing the CDW correlations. For a modestly strong attractive V_{pd}, the SC correlations become quasi-long-ranged with a divergent PDW susceptibility.

I. INTRODUCTION

The pair density wave (PDW) is a novel superconducting (SC) state in which the Cooper pairs carry finite center-of-mass momentum and the SC order parameter varies periodically in space in such a way that its spatial average vanishes [1–4]. The first example of PDW is the Fulde-Ferrell-Larkin-Ovchinnikov state in which the PDW state is more stable than the spatially uniform SC state when the Fermi surfaces are split by an external magnetic field [5, 6]. The PDW state has been discussed as a leading candidate state to understand the physics of cuprate high-temperature superconductors and other strongly correlated systems, where it has been proposed that various phases, including the unconventional superconductivity, charge density wave (CDW) and spin density wave (SDW) orders, can emerge by partially melting the PDW state [2–4, 7]. Recently, intense interest in the PDW state has emerged due to experimental observations in underdoped cuprate superconductors, where signatures of PDW states have been observed via local Cooper pair tunneling and scanning tunneling microscopy in underdoped $Bi_2Sr_2CaCu_2O_{8+x}$ (BSCCO) [8–11] and the dynamical inter-layer decoupling in $La_{1.875}Ba_{0.125}CuO_4$ (LBCO) [12–18]. Signatures of PDW states have also been reported in kagome superconductor CsV_3Sb_5 [19] and monolayer iron-based high-Tc Fe(Te,Se) films [20].

While much is known about the properties of the PDW state [1–4, 16, 17, 21], there are very few microscopic models which are shown to have PDW ground states [22–29] and especially no PDW long-range order has been established in unbiased calculations in two or higher dimensions. These include the one-dimensional (1D) Kondo-Heisenberg model [22], the extended Hubbard-Heisenberg model on two-leg ladder [23], generalized t-J

and Hubbard models [24–27] and strong coupling limit of Holstein-Hubbard model [28, 29]. However, even in quasi-1D systems such as ladders, no reported evidence of PDW quasi-long-range order with divergent susceptibility – the closest one can have to PDW long-range order – in standard Hubbard model on any systems including two-leg ladder, especially that are closely related to real materials.

In the present work, we consider the three-band Hubbard model (also known as the Emery model) on the square lattice, which has long been proposed as one of the minimal models to describe the properties of cuprate high-temperature superconductors [30–34], with the goal of determining whether this model supports PDW order. We employ density-matrix renormalization group (DMRG) [35] to study the lightly hole doped three-band Hubbard model [33] on long two-leg square cylinders. Our main results are that the ground state of the system is consistent with that of a PDW state with power-law and mutually commensurate SC, CDW and SDW correlations. The SC correlations oscillate periodically and change sign in real space. The PDW ordering wavevector $Q \approx 2\pi\delta$ is incommensurate and hole doping density δ dependent. The Cooper pairing is dominant between neighboring Cu sites with d-wave symmetry. Interestingly, we find that near-neighbor attractions, especially V_{pd} between neighboring Cu and O sites, can notably enhance the SC correlations while suppressing the CDW correlations. For modestly strong near-neighbor attractions, the SC correlations become quasi-long-ranged with a divergent PDW susceptibility.

II. MODEL AND METHOD

The lattice structure and the parameters of the three-band Hubbard model on the 2-leg square cylinder are shown in Fig.1 where unit cell has a Cu $3d_{x^2-y^2}$ (Cu) orbital and oxygen $2p_x/2p_y$ (Ox/Oy) orbitals. Following
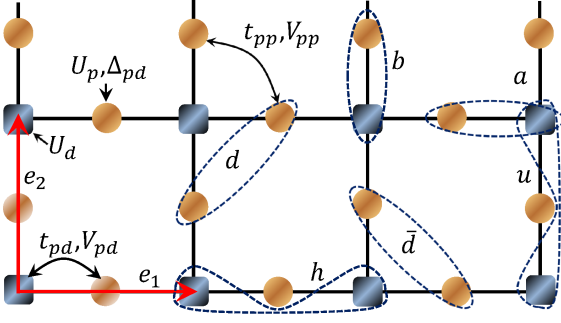
[*] hcjiang@stanford.edu

FIG. 1. Three-band Hubbard model on square lattice. The squares represent Cu $d_{x^2-y^2}$ orbitals and circles represent O $2p_x/p_y$ orbitals. U_d and U_p are onsite Cu and O Coulomb interactions, V_{pd} and V_{pp} are near-neighbor Cu-O and O-O Coulomb interactions, t_{pd} and t_{pp} are near-neighbor Cu-O and O-O hole hopping matrix elements. Δ_{pd} is the energy difference between having a hole on the O versus Cu sites. $e_1 = (1,0)$ and $e_2 = (0,1)$ are lattice basis vectors. The dashed loops represent bonds a, b, d, $\bar{d}$, h and u.

Ref.[33], we consider the hole representation where the Hamiltonian is defined as

$$
\begin{aligned}
H = & -t_{pd} \sum_{\langle ij \rangle \sigma} (\hat{d}_{i\sigma}^+ \hat{p}_{j\sigma} + h.c.) - t_{pp} \sum_{\langle ij \rangle \sigma} (\hat{p}_{i\sigma}^+ \hat{p}_{j\sigma} + h.c.) \\
& + U_d \sum_i \hat{n}_{i\uparrow}^d \hat{n}_{i\downarrow}^d + U_p \sum_i \hat{n}_{i\uparrow}^p \hat{n}_{i\downarrow}^p + \Delta_{pd} \sum_{i\sigma} \hat{p}_{i\sigma}^+ \hat{p}_{i\sigma} \\
& + V_{pd} \sum_{\langle ij \rangle} \hat{n}_i^d \hat{n}_j^p + V_{pp} \sum_{\langle ij \rangle} \hat{n}_i^p \hat{n}_j^p.
\end{aligned}
\tag{1}
$$

Here $\hat{d}_{i\sigma}^+$ and $\hat{p}_{j\sigma}^+$ create holes with spin-σ on the ith Cu and j^{th} oxygen sites, and $\langle ij \rangle$ denotes nearest-neighbor (NN) sites. $\hat{n}_{i\sigma}^d = \hat{d}_{i\sigma}^+ \hat{d}_{i\sigma}$ and $\hat{n}_{i\sigma}^p = \hat{p}_{i\sigma}^+ \hat{p}_{i\sigma}$ are number operators and $\hat{n}_i^{d/p} = \sum_\sigma \hat{n}_{i\sigma}^{d/p}$. $\Delta_{pd} = \epsilon_p - \epsilon_d$ is the energy difference between having a hole on the O site (ϵ_p) versus a Cu site (ϵ_d). t_{pd} and t_{pp} are the hole hopping matrix elements between NN Cu and O sites and NN O sites. U_d and U_p are the on-site Cu and O Coulomb repulsion, V_{pd} and V_{pp} are NN Cu-O and O-O interactions. Following [33], we have fixed the phases of orbitals such that the signs of hopping matrix elements remain the same throughout the lattice and are positive [36]. We set $t_{pd} = 1$ as the energy unit and take a canonical set of parameters $t_{pp} = 0.5$, $U_d = 8$, $U_p = 3$, $\Delta_{pd} = 3$ for cuprates [33, 37, 38]. We study the ground state properties of the system as a function of V_{pd} and V_{pp}.

In the present study, we take the lattice geometry to be cylindrical with periodic/open boundary condition in the e_2/e_1 direction, as shown in Fig.1. We focus on two-leg cylinders with width $L_y = 2$ and length up to $L_x = 96$, where L_x and L_y are the number of unit cells in the e_1 and e_2 directions, respectively. The total number of sites is $N = 3L_x L_y + 2L_y = 3N_u + 2L_y$, where N_u is the number of unit cell. The overall hole density of the system is defined as $\rho = 1 + \delta$, where $\delta = N_h/N_u$ [39] and N_h denote the hole doping concentration and number of doped

holes away from half-filling, respectively. We consider both $\delta = 1/12$ and $\delta = 1/8$ hole doping concentrations and perform up to 157 sweeps and keep up to $m = 25000$ number of states with a typical truncation error $\epsilon \sim 10^{-9}$.

III. SUPERCONDUCTING CORRELATION

To test the possibility of superconductivity, we calculate the equal-time SC pair-field correlations. As the ground state with an even number of holes always have total spin 0, we focus on spin-singlet SC correlation [40], which is defined as

$$
\Phi_{\alpha\beta}(r) = \langle \hat{\Delta}_\alpha^\dagger(x_0, y_0) \hat{\Delta}_\beta(x_0 + r, y_0) \rangle.
\tag{2}
$$

Here, $\hat{\Delta}_\alpha^\dagger(x, y) = \frac{1}{\sqrt{2}} [\hat{c}_{(x,y),\uparrow}^\dagger \hat{c}_{(x,y)+\alpha,\downarrow}^\dagger - \hat{c}_{(x,y),\downarrow}^\dagger \hat{c}_{(x,y)+\alpha,\uparrow}^\dagger]$ is spin-singlet pair creation operator on the bond $\alpha = a$, b, d, h and u defined in Fig.1. (x_0, y_0) is a reference bond with $x_0 \sim L_x/4$, r is the distance between two bonds in the e_1 direction. We have calculated different components of the SC correlations, including Φ_{aa}, Φ_{ab}, Φ_{bb}, $\Phi_{dd}(r)$, $\Phi_{d\bar{d}}(r)$, $\Phi_{\bar{d}\bar{d}}(r)$, Φ_{hh}, Φ_{uu} and Φ_{uh} and find that $\Phi_{hh}(r)$ and $\Phi_{uu}(r)$ exhibit the strongest SC correlations as shown in Fig.2A, i.e. the pairing is dominant between neighboring Cu sites. The pairing symmetry is consistent with d-wave, which is characterized by the fact $\Phi_{uu}(r) \sim \Phi_{hh}(r) \sim -\Phi_{uh}(r)$.

The spatial distribution of SC correlations $\Phi_{hh}(r)$ for the three representative choices of parameters are shown in Fig.2C-D: $\Phi_{hh}(r)$ exhibits clear spatial oscillations which can be well fitted by $\mathbf{\Phi_{hh}(r)} \sim \mathbf{f(r)}\phi_{hh}(\mathbf{r})$ for a large region of r, where $f(r)$ sets the envelope and $\phi_{hh}(r)$ determines the spatial oscillation. At long distances, the envelope function $f(r)$ is consistent with a power-law decay $\mathbf{f(r)} \propto \mathbf{r^{-K_{sc}}}$ with a Luttinger exponent K_{sc} [41]. For instance, the extracted exponent $K_{sc} = 3.4(2)$ at $V_{pd} = 1.0$ and $V_{pp} = 0.75$, $K_{sc} = 2.4(1)$ at $V_{pd} = 0$ and $V_{pp} = 0$, and $K_{sc} = 1.80(8)$ at $V_{pd} = -1.0$ even $V_{pp} = 0$. It is worth emphasizing that the SC correlations can be notably enhanced by either reducing the NN repulsion or increasing the NN attraction, which is similar to the single-band Hubbard model [42–44]. This is directly supported by the SC correlation in Fig.2B and the value of K_{sc} mentioned above. More complete results of K_{sc} for Φ_{hh} and Φ_{uu} at $\delta = 1/8$ and $\delta = 1/12$ are shown in Fig.3A. This shows that the static PDW susceptibility diverges as $\chi_{pdw} \sim T^{-(2-K_{sc})}$ since $K_{sc} < 2$ as $T \to 0$. As far as we know, to date, this is the strongest indication of PDW order that has been found in any DMRG study in doped Hubbard model on the square lattice.

The spatial oscillation of the SC correlations $\Phi(r)$ is characterized by the normalized function $\phi(r) = \Phi(r)/f(r)$ as mentioned above. Examples of $\phi_{hh}(r)$ for the representative choices of parameters are in Fig.2C-D for $\delta = 1/8$ and $\delta = 1/12$, respectively. It is clear that $\phi_{hh}(r)$ oscillates periodically in real space and can be well fitted by $\phi_{\mathbf{hh}}(\mathbf{r}) \sim \sin(\mathbf{Qr} + \theta)$, which is
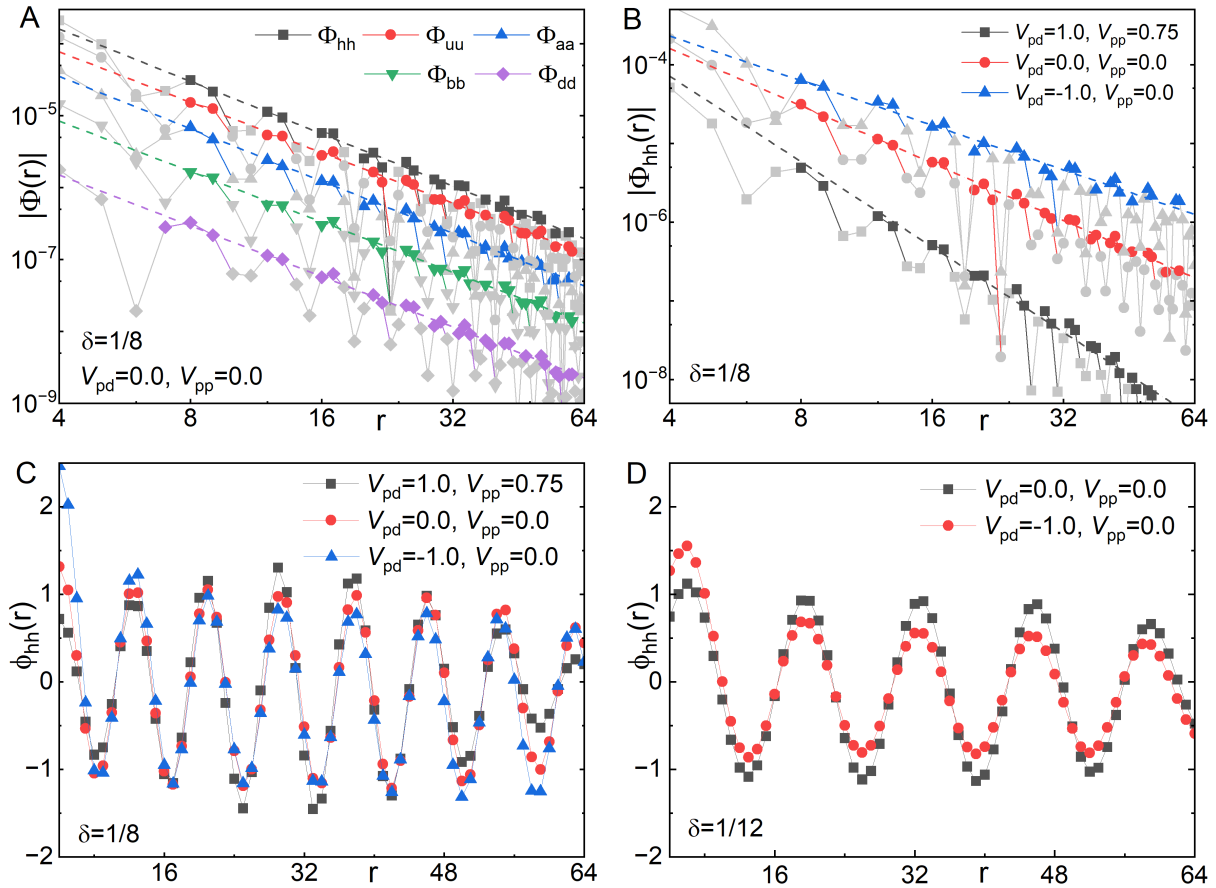
FIG. 2. Superconducting correlations. The magnitude of SC correlations $|\Phi_{\alpha\beta}(r)|$ are shown in (A) and $|\Phi_{hh}(r)|$ are shown in (B). The dashed lines represent fits to a power-law function $f(r) = A * r^{-K_{sc}}$. Data points away from the envelope and those at short distances are discarded in the fitting process and are shown in gray color. The normalized function $\phi_{hh}(r) = \Phi_{hh}(r)/f(r)$ reflect the spatial oscillation of $\Phi_{hh}(r)$ for $\delta = 1/8$ in (C) and $\delta = 1/12$ in (D).

consistent with that of a PDW state [4]. The PDW ordering wavevector Q is incommensurate and hole doping dependent as $Q \approx 2\pi\delta$, corresponding to a wavelength $\lambda_{sc} \approx 1/\delta$, e.g., $\lambda_{sc} \approx 8$ at $\delta = 1/8$ and $\lambda_{sc} \approx 12$ at $\delta = 1/12$ as shown in Fig.2C-D. This is distinct with $Q \approx 4\pi\delta$ in a qualitatively different system [25].

IV. CHARGE DENSITY WAVE ORDER

To describe the charge density properties of the ground state of the system, we have calculated the charge density profile $n_\alpha(x, y) = \langle \hat{n}_\alpha(x, y) \rangle$ and its local rung average $n(x) = \sum_{y=1}^{L_y} n_a(x, y)/L_y$, where α=Cu/Ox/Oy site. Different from the single-band Hubbard model on square lattice [45–49], the spatial oscillation of $n_\alpha(x)$ in the three-band Hubbard model is characterized by two wavevectors at Q and $2Q$, corresponding to wavelengths $\lambda_Q \approx 1/\delta$ and $\lambda_{2Q} \approx 1/2\delta$, respectively. Examples of $n_{cu}(x)$ and $n_{oy}(x)$ for two representative sets of parameters are shown in Fig.4A-B.

At long distances, the spatial decay of the CDW correlation is dominated by a power-law with Luttinger exponent K_c, which can be obtained by fitting the charge density oscillations (Friedel oscillations) induced by the boundaries of the cylinder [50]

$$\mathbf{n}_\alpha(\mathbf{x}) = \mathbf{A_Q} * \cos(\mathbf{Qx} + \phi_1) * \mathbf{x}^{-\mathbf{K_c}(\alpha)/2} \quad (3)$$
$$+ \mathbf{A_{2Q}} * \cos(\mathbf{2Qx} + \phi_2) * \mathbf{x}^{-\mathbf{K_c}(\alpha)/2} + \mathbf{n_0}(\alpha).$$

Here A_Q and A_{2Q} are CDW amplitudes, ϕ_1 and ϕ_2 are phase shifts, n_0 is the mean density, and $Q \approx 2\pi\delta$. Similar with the single-band Hubbard model on four-leg square cylinders [43], we find that the CDW strength can be notably suppressed by NN attraction evidenced by the monotonic increase of K_c with the increase of NN attraction $|V_{pd}|$ in Fig.3B. Examples of K_c at $\delta = 1/8$ and $V_{pp} = 0$ are $K_c(\text{Cu})=2.29(5)$ and $K_c(\text{Oy})=2.25(5)$ for $V_{pd}=0$, and $K_c(\text{Cu})=2.52(7)$ and $K_c(\text{Oy})=2.54(7)$ for $V_{pd}=-1$. More complete results are shown in Fig.3B.

Interestingly, we find that the NN attraction can notably enhance the charge oscillation at Q while suppressing the charge oscillation at $2Q$, evidenced by the
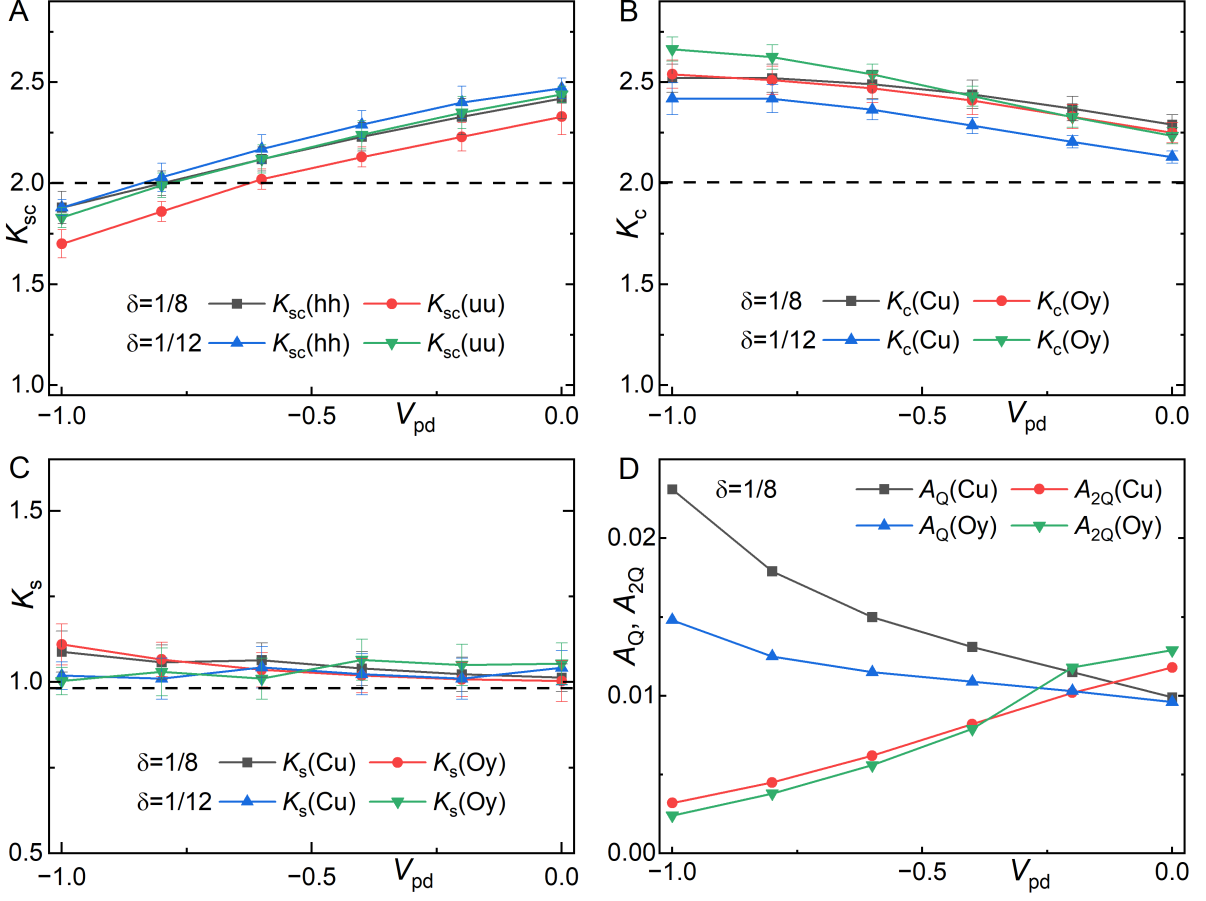
FIG. 3. Luttinger exponents and CDW amplitudes. Extracted exponents K_{sc} in (A), K_c in (B), K_s in (C), and CDW amplitudes A_Q and A_{2Q} in (D) as a function of V_{pd} with $V_{pp} = 0$. Error bars denote the numerical uncertainty and dash lines are guides for eyes.

CDW amplitudes A_Q and A_{2Q} as shown in Fig.3D. The competition between the charge oscillation at $2Q$ and SC correlation arises from the interplay between electron correlation and electron itinerancy, where the NN electron attraction promotes superconductivity but suppresses charge oscillation. The relationship between charge oscillation at Q and SC correlation remains more intriguing. It may be possible that there is a small but finite uniform SC component Δ_0, so that the charge oscillation $\Delta_Q^P \Delta_0^*$ at Q, can be notably intensified by the NN electron attraction, just as the SC correlation is enhanced by the same attraction. The charge oscillation is dominant at $2Q$ for strong NN repulsion, e.g., $A_{2Q} \approx 10 A_Q$ at $V_{pd} = 1.0$ and $V_{pp} = 0.75$. When the NN interaction is weak, the charge oscillations at both Q and $2Q$ become comparable with each other, e.g., $A_{2Q} \approx A_Q$ at $V_{pd} = V_{pp} = 0$ in Fig.3D. However, when the NN interactions become attractive, e.g., $V_{pd} \leq -0.2$ in Fig.3D, the charge oscillation at Q becomes dominant, e.g., $A_Q \gtrsim 6 A_{2Q}$ at $V_{pd} = -1$ and $V_{pp} = 0$.

V. SPIN-SPIN CORRELATION

To describe the magnetic properties of the ground state, we calculate the spin-spin correlation functions $F_\alpha(r) = \langle \vec{S}_{(x_0, y_0)} \cdot \vec{S}_{(x_0+r, y_0)} \rangle$, where α=Cu/Ox/Oy site. Fig.4C show examples of $F_{Cu}(r)$ and $F_{Oy}(r)$ for two representative choices of parameters where we find that the spin-spin correlations between Cu sites are dominant evidenced by $|F_{Cu}(r)| \gg |F_{Oy}(r)| \sim |F_{Ox}(r)|$. Contrary to the exponential decaying spin-spin correlation in the Luther-Emery liquid of the square lattice single-band Hubbard model [47–49, 51, 52], we find that $F(r)$ in the lightly doped three-band Hubbard model decays as a power-law $\mathbf{F}_\alpha(\mathbf{r}) \propto \mathbf{r}^{-\mathbf{K_s}(\alpha)}$ at long distances, with a Luttinger exponent $K_s \sim 1$. For instance, $K_s(\text{Cu})=1.09(6)$ and $K_s(\text{Oy})=1.11(6)$ for V_{pd}=-1 and V_{pp}=0 at $\delta = 1/8$. More complete results are shown in Fig.3C. Consistent with a PDW state, we find that $F(r)$ exhibits clear spatial oscillation as shown in Fig.4D at the PDW ordering wavevector Q with a wavelength $\lambda_s \approx \lambda_{sc} \approx 1/\delta$, i.e., $\lambda_s \approx 8$ at $\delta = 1/8$.
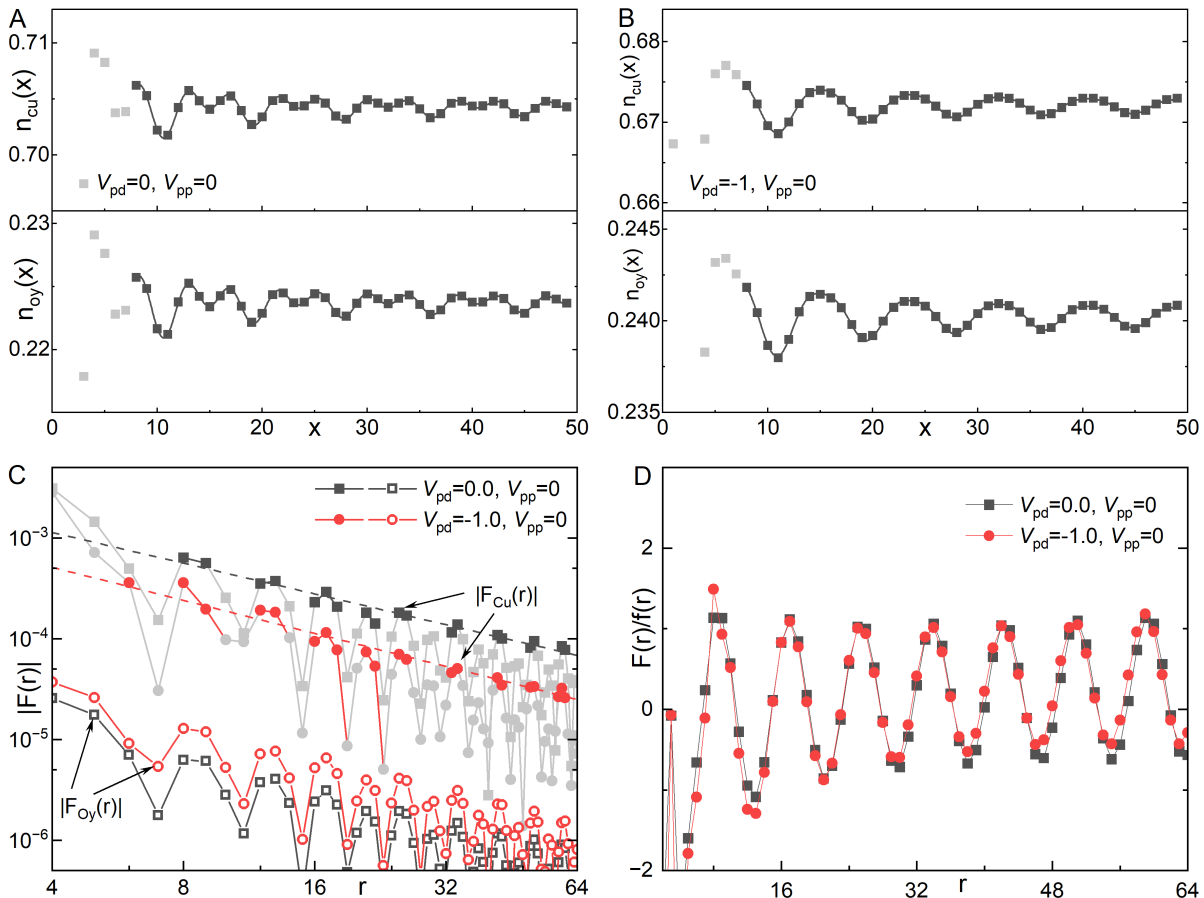
FIG. 4. Charge density profile and spin-spin correlations. Charge density profiles $n_{cu}(x)$ and $n_{oy}(x)$ in (A) for $V_{pd} = 0$ and (B) for $V_{pd} = -1$. The solid lines denote fittings using Eq.(3). The magnitude of spin-spin correlations $|F(r)|$ in (C) and its normalized function in (D). The dashed lines represent fits to a power-law function $f(r) = A * r^{-K_s}$. Here $\delta = 1/8$ and data points away from the envelope and those at short distances are discarded in gray color in the fitting process.

VI. ENTANGLEMENT ENTROPY

Our results suggest that there are multiple gapless modes including charge and spin with a central charge c which can be obtained by calculating the von Neumann entropy $S(x) = -\mathrm{Tr}\rho_x \ln \rho_x$, where ρ_x is the reduced density matrix of a subsystem of length x. For critical systems in 1+1 dimensions described by a conformal field theory, it has been established[53, 54] that for an open system of length L_x,

$$
\begin{aligned}
S(x) &= \frac{c}{6} \ln \left[\frac{4(L_x + 1)}{\pi} \sin \frac{\pi(2x+1)}{2(L_x+1)} |\sin k_F| \right] \\
&+ \tilde{A} \frac{\sin[k_F(2x+1)]}{\frac{4(L_x+1)}{\pi} \sin \frac{\pi(2x+1)}{2(L_x+1)} |\sin k_F|} + \tilde{S},
\end{aligned} \tag{4}
$$

where $\tilde{A}$ and $\tilde{S}$ are fitting parameters, and k_F is the Fermi momentum. We find that the extracted $c \approx 2$ with examples shown in Fig.5. This suggests that there is one gapless charge mode and one gapless spin mode.

VII. SUMMARY AND DISCUSSION

In summary, we have studied the ground state properties of hole-doped three-band Hubbard model on two-leg square cylinders with NN Cu-O and O-O interactions. Based on our results, we conclude that the ground state of the system is consistent with that of a PDW state, with mutually commensurate and power-law SC, CDW and SDW correlations. The Cooper pairing is dominant between neighboring Cu sites with d-wave symmetry. For modestly strong NN attraction, quasi-long-range PDW order with a divergent susceptibility emerges. As the critical attraction, where PDW quasi-long-range order develops, is close to that identified recently in cuprate $Ba_{2-x}Sr_xCuO_{3+\delta}$ [42], it may be reasonable to expect a comparable effective NN attraction in the CuO_2 plane given their chemical similarity.

When the NN attraction $V_{pd} \leq -0.2$ as shown in Fig.3D, it is clear that the CDW at wavevector Q (Q-CDW) is dominant while the CDW at $2Q$ ($2Q$-CDW) is secondary. It is worth noting that our results suggest
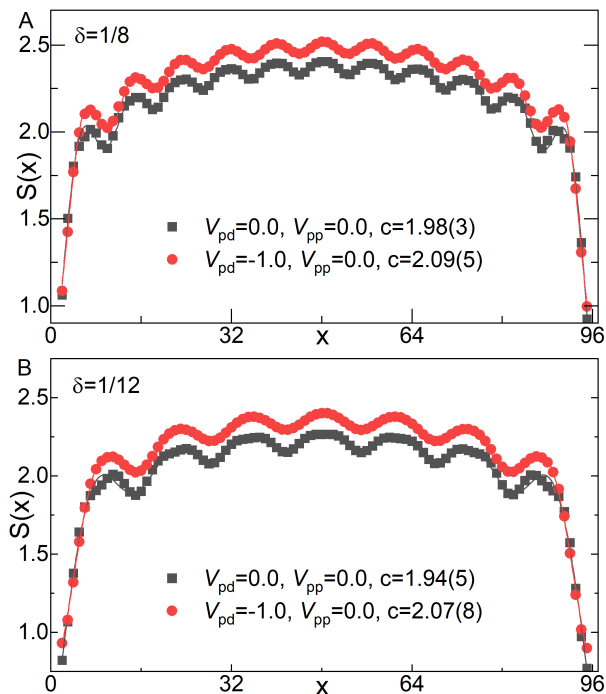
FIG. 5. Entanglement entropy. Von Neumann entanglement entropy $S(x)$ at $\delta = 1/8$ in (A) and $\delta = 1/12$ in (B). A couple of data points in gray color close to the open ends are excluded in the fitting to minimize the boundary effect.

that the uniform SC component may be absent or at least small. If there was a small uniform component Δ_0, then a Q-CDW could be generated by the product $\Delta_Q^P \Delta_0^*$ with PDW order Δ_Q^P. Accordingly, the 2Q-CDW could be generated by the product of PDW with itself $\Delta_Q^P \Delta_{-Q}^{P*}$. If this is the case, then the Q-CDW should be small as the uniform component is small, while the 2Q-CDW should be dominant. However, this is contrary to our observations especially when $V_{pd} \leq -0.2$. Alternatively, the 2Q-CDW could come from a composite of two SDW at Q, which is, however, inconsistent with our observations. This is because the 2Q-CDW weakens notably with the increase of NN attraction when $V_{pd} \leq -0.2$, while the SDW remains unchanged. Although the favored forms of order, with SC and SDW at the same Q, and CDW at both Q and 2Q, are reminiscent of those conjectured to be present in the cuprates BSCCO and LBCO [10–12, 16, 17], it is worth emphasizing that the underlying mechanism of our observations that all three orders (PDW, CDW and SDW) are all at the same Q can be very different from the stripe picture of PDW [4].

[1] E. Berg, E. Fradkin, S. A. Kivelson, and J. M. Tranquada, Striped superconductors: how spin, charge and superconducting orders intertwine in the cuprates, New J. Phys. **11**, 115004 (2009).

[2] P. A. Lee, Amperean pairing and the pseudogap phase of cuprate superconductors, Phys. Rev. X **4**, 031017 (2014).

[3] E. Fradkin, S. A. Kivelson, and J. M. Tranquada, Colloquium: Theory of intertwined orders in high temperature superconductors, Rev. Mod. Phys. **87**, 457 (2015).

[4] D. F. Agterberg, J. S. Davis, S. D. Edkins, E. Fradkin, D. J. Van Harlingen, S. A. Kivelson, P. A. Lee, L. Radzihovsky, J. M. Tranquada, and Y. Wang, The physics of pair-density waves: Cuprate superconductors and beyond, Annual Review of Condensed Matter Physics **11**, 231 (2020), and references therein.

[5] P. Fulde and R. A. Ferrell, Superconductivity in a strong spin-exchange field, Phys. Rev. **135**, A550 (1964).

[6] A. I. Larkin and Y. N. Ovchinnikov, Nonuniform state of superconductors, Sov. Phys. JETP **20**, 762 (1965).

[7] A. Himeda, T. Kato, and M. Ogata, Stripe states with spatially oscillating d-wave superconductivity in the two-dimensional $t - t^{'} - J$ model, Phys. Rev. Lett. **88**, 117001 (2002).

[8] M. H. Hamidian, S. D. Edkins, S. H. Joo, A. Kostin, H. Eisaki, S. Uchida, M. J. Lawler, E.-A. Kim, A. P. Mackenzie, K. Fujita, J. Lee, and J. C. S. Davis, Detection of a cooper-pair density wave in Bi$_2$Sr$_2$CaCu$_2$O$_{8+x}$, Nature **532**, 343 (2016).

[9] W. Ruan, X. Li, C. Hu, Z. Hao, H. Li, P. Cai, X. Zhou, D.-H. Lee, and Y. Wang, Visualization of the periodic modulation of cooper pairing in a cuprate superconductor, Nature Physics , 1178 (2018).

[10] S. D. Edkins, A. Kostin, K. Fujita, A. P. Mackenzie, H. Eisaki, S. Uchida, S. Sachdev, M. J. Lawler, E.-A. Kim, J. C. Séamus Davis, and M. H. Hamidian, Magnetic field–induced pair density wave state in the cuprate vortex halo, Science **364**, 976 (2019).

[11] X. Liu, Y. X. Chong, R. Sharma, and J. C. S. Davis, Discovery of a cooper-pair density wave state in a transition-metal dichalcogenide, Science **372**, 1447 (2021).

[12] Q. Li, M. Hücker, G. D. Gu, A. M. Tsvelik, and J. M. Tranquada, Two-Dimensional Superconducting Fluctuations in Stripe-Ordered La$_{1.875}$Ba$_{0.125}$CuO$_4$, Phys. Rev. Lett. **99**, 067001 (2007).

[13] D. F. Agterberg and H. Tsunetsugu, Dislocations and vortices in pair-density-wave superconductors, Nature Physics , 639 (2008).

[14] E. Berg, E. Fradkin, E.-A. Kim, S. A. Kivelson, V. Oganesyan, J. M. Tranquada, and S. C. Zhang, Dynamical layer decoupling in a stripe-ordered high-T$_c$ superconductor, Phys. Rev. Lett. **99**, 127003 (2007).

[15] J. M. Tranquada, G. D. Gu, M. Hücker, Q. Jie, H.-J. Kang, R. Klingeler, Q. Li, N. Tristan, J. S. Wen, G. Y. Xu, Z. J. Xu, J. Zhou, and M. v. Zimmermann, Evi-

dence for unusual superconducting correlations coexisting with stripe order in $La_{1.875}Ba_{0.125}CuO_4$, Phys. Rev. B **78**, 174529 (2008).

[16] J. M. Tranquada, Cuprate superconductors as viewed through a striped lens, Advances in Physics **69**, 437 (2020).

[17] J. M. Tranquada, Topological doping and superconductivity in cuprates: An experimental perspective, Symmetry **13**, 2365 (2021).

[18] P. M. Lozano, T. Ren, G. D. Gu, A. M. Tsvelik, J. M. Tranquada, and Q. Li, Testing for pair-density-wave order in $La_{1.875}Ba_{0.125}CuO_4$, arXiv:2110.05513 (2021).

[19] H. Chen, H. Yang, B. Hu, Z. Zhao, J. Yuan, Y. Xing, G. Qian, Z. Huang, G. Li, Y. Ye, S. Ma, S. Ni, H. Zhang, Q. Yin, C. Gong, Z. Tu, H. Lei, H. Tan, C. Zhou, S.and Shen, X. Dong, B. Yan, Z. Wang, and H. J. Gao, Roton pair density wave in a strong-coupling kagome superconductor, Nature **599**, 222–228 (2021).

[20] Y. Liu, T. Wei, G. He, Y. Zhang, Z. Wang, and J. Wang, Discovery of a pair density wave state in a monolayer high-T_c iron-based superconductor, arXiv:2209.04592 (2022).

[21] Y.-M. Wu, P. A. Nosov, A. A. Patel, and S. Raghu, Pair density wave order from electron repulsion, arXiv:2209.09254 (2022).

[22] E. Berg, E. Fradkin, and S. A. Kivelson, Pair-density-wave correlations in the kondo-heisenberg model, Phys. Rev. Lett. **105**, 146403 (2010).

[23] A. Jaefari and E. Fradkin, Pair-density-wave superconducting order in two-leg ladders, Phys. Rev. B **85**, 035104 (2012).

[24] J. Venderley and E.-A. Kim, Evidence of pair-density wave in spin-valley locked systems, Science Advances **5**, eaat4698 (2019).

[25] X. Y. Xu, K. T. Law, and P. A. Lee, Pair Density Wave in the Doped $t − J$ Model with Ring Exchange on a Triangular Lattice, Phys. Rev. Lett. **122**, 167001 (2019).

[26] C. Peng, Y.-F. Jiang, T. P. Devereaux, and H.-C. Jiang, Precursor of pair-density wave in doping kitaev spin liquid on the honeycomb lattice, npj Quantum Mater. **6**, 64 (2021).

[27] C. Peng, Y.-F. Jiang, Y. Wang, and H.-C. Jiang, Gapless spin liquid and pair density wave of the hubbard model on three-leg triangular cylinders, New Journal of Physics **23**, 123004 (2021).

[28] Z. Han, S. A. Kivelson, and H. Yao, Strong coupling limit of the holstein-hubbard model, Phys. Rev. Lett. **125**, 167001 (2020).

[29] K. S. Huang, Z. Han, S. A. Kivelson, and H. Yao, Pair-density-wave in the strong coupling limit of the holstein-hubbard model, npj Quantum Mater. **7**, 17 (2022).

[30] J. Zaanen, G. A. Sawatzky, and J. W. Allen, Band gaps and electronic structure of transition-metal compounds, Phys. Rev. Lett. **55**, 418 (1985).

[31] V. J. Emery, Theory of high-T_c superconductivity in oxides, Phys. Rev. Lett. **58**, 2794 (1987).

[32] F. C. Zhang and T. M. Rice, Effective Hamiltonian for the superconducting Cu oxides, Phys. Rev. B **37**, 3759 (1988).

[33] S. R. White and D. J. Scalapino, Doping asymmetry and striping in a three-orbital CuO_2 Hubbard model, Phys. Rev. B **92**, 205112 (2015).

[34] E. W. Huang, C. B. Mendl, S. Liu, S. Johnston, H.-C. Jiang, B. Moritz, and T. P. Devereaux, Numerical evidence of fluctuating stripes in the normal state of high-Tc cuprate superconductors, Science **358**, 1161 (2017).

[35] S. R. White, Density matrix formulation for quantum renormalization groups, Phys. Rev. Lett. **69**, 2863 (1992).

[36] This is equivalent to the usual three-band Hubbard model after a gauge transformation with the same ground state properties including correlations.

[37] N. P. Armitage, P. Fournier, and R. L. Greene, Progress and perspectives on electron-doped cuprates, Rev. Mod. Phys. **82**, 2421 (2010).

[38] K. Haule, T. Birol, and G. Kotliar, Covalency in transition-metal oxides within all-electron dynamical mean-field theory, Phys. Rev. B **90**, 075136 (2014).

[39] Although $N \neq 3N_u$ such that the average value of δ differs slightly from $\bar{\delta} = 3N_h/N$, deep in the bulk, i.e., relatively far from the open boundaries, $\delta = \bar{\delta}$.

[40] We have also calculated the spin-triplet SC correlations, which are much weaker than the spin-singlet SC correlations. This is expected as the ground state of the system is a spin-singlet state.

[41] T. D. Kühner, S. R. White, and H. Monien, One-dimensional bose-hubbard model with nearest-neighbor interaction, Phys. Rev. B **61**, 12474 (2000).

[42] Z. Chen, Y. Wang, S. N. Rebec, T. Jia, M. Hashimoto, D. Lu, B. Moritz, R. G. Moore, T. P. Devereaux, and Z.-X. Shen, Anomalously Strong Near-Neighbor Attraction in Doped 1D Cuprate Chains, Science **373**, 1235 (2021).

[43] C. Peng, Y. Wang, J. Wen, Y. Lee, T. Devereaux, and H.-C. Jiang, Enhanced superconductivity by near-neighbor attraction in the doped hubbard model, arXiv:2206.03486 (2022).

[44] D.-W. Qu, B.-B. Chen, H.-C. Jiang, Y. Wang, and W. Li, Spin-triplet pairing induced by near-neighbor attraction in the cuprate chain, arXiv:2110.00564 (2021).

[45] S. R. White and D. J. Scalapino, Ground states of the doped four-leg t-J ladder, Phys. Rev. B **55**, R14701 (1997).

[46] B.-X. Zheng, C.-M. Chung, P. Corboz, G. Ehlers, M.-P. Qin, R. M. Noack, H. Shi, S. R. White, S. Zhang, and G. K.-L. Chan, Stripe Order in the Underdoped Region of the Two-Dimensional Hubbard Model, Science **358**, 1155 (2017).

[47] H.-C. Jiang and T. P. Devereaux, Superconductivity in the doped hubbard model and its interplay with next-nearest hopping t', Science **365**, 1424 (2019).

[48] Y.-F. Jiang, J. Zaanen, T. P. Devereaux, and H.-C. Jiang, Ground state phase diagram of the doped hubbard model on the four-leg cylinder, Phys. Rev. Research **2**, 033073 (2020).

[49] H.-C. Jiang, S. Chen, and Z.-Y. Weng, Critical role of the sign structure in the doped mott insulator: Luther-emery versus fermi-liquid-like state in quasi-one-dimensional ladders, Phys. Rev. B **102**, 104512 (2020).

[50] S. R. White, I. Affleck, and D. J. Scalapino, Friedel oscillations and charge density waves in chains and ladders, Phys. Rev. B **65**, 165122 (2002).

[51] H.-C. Jiang, Z.-Y. Weng, and S. A. Kivelson, Superconductivity in the doped t-J model: Results for four-leg cylinders, Phys. Rev. B **98**, 140505 (2018).

[52] C.-M. Chung, M. Qin, S. Zhang, U. Schollwöck, and S. R. White (The Simons Collaboration on the Many-Electron Problem), Plaquette versus ordinary d-wave pairing in the $t^{'}$-Hubbard model on a width-4 cylinder, Phys. Rev.

B **102**, 041106 (2020).

[53] P. Calabrese and J. Cardy, Entanglement entropy and quantum field theory, J. Stat. Mech. Theory Exp. **2004**, P06002 (2004).

[54] M. Fagotti and P. Calabrese, Universal parity effects in the entanglement entropy of XX chains with open boundary conditions, J. Stat. Mech. Theory Exp. **2011**, P01017 (2011).